Research Article

Mechanics Design of Conical Spiral Structure for Flexible Coilable Antenna Array

Hairui Wang,[1,2] Yao Zhang,[1] Siyu Chen,[1] Yinji Ma,[1] Heling Wang,[3] Ying Chen ●,[3] and Xue Feng[1]

[1]*AML, Department of Engineering Mechanics, Center for Flexible Electronics Technology, Tsinghua University, Beijing 100084, China*
[2]*State Key Laboratory for Strength and Vibration of Mechanical Structures, Xi'an Jiaotong University, Xi'an 710049, China*
[3]*Institute of Flexible Electronics Technology of THU, Jiaxing 314000, China*

Correspondence should be addressed to Ying Chen; chenying@ifet-tsinghua.org

Limited by the effective launch capacity of a rocket, the deployable antenna is very important in the design of spaceborne antenna array. Compared to traditional deployable antenna, flexible coilable antenna array has higher surface precision and better vibration control and therefore is more suitable for high frequency communication. In order to minimize the weight of satellite and reduce cost of its launch, a design guideline to the geometry parameters of flexible coilable antenna array is crucial. Existing models cannot be directly applied to interaction and large deformation between coilable membrane and conical spiral antenna in the flexible coilable antenna array. Hence, the geometry parameters of the conical spiral structure and the thickness of the coilable membrane in the flexible coilable antenna array have not been optimized yet. In this paper, the interaction between the coilable membrane and the concial spiral antenna is analyzed in the antenna array. A concise formula is derived to predict the critical force that flattens the conical spiral antenna by a coiling scroll. Combined with a theoretical model to predict the deformation of the membrane, the model provides an important theoretical support for the lightweight design and mechanical design of flexible coilable antenna array, such as the thickness of the coilable membrane. The proposed design is validated by experiments. The above findings have potential applications in the effective reduction of antenna array weight and satellite launch costs.

1. Introduction

Antenna is an important terminal in information transmission system [1–4]. Limited by the effective launching capacity of the rocket, the existing large-scale spaceborne antenna array is usually folded to reduce the space occupied at the launching stage [5–8] and then deployed in orbit and responsible for communication transmission. For example, tensegrity-membrane and umbrella antenna have been put into use on the satellite [9–11]. Due to folding traces on the antenna surface, these folded antennas have problems such as large overall weight and poor shape accuracy [12–15]. Hence, it is difficult to apply in high-frequency communication which requires strict control of membrane deformation and vibration [16–18]. Inspired by serpentine design with low strain in two-dimensional (2D) flexible electronics [19–22], flexible coilable antenna array with 2D patch antennas can overcome the above problems [23]. However, the 2D patch antenna behaving linear polarization cannot handle the ionosphere of the atmosphere compared with 3D spiral antennas behaving circular polarization [24]. Hence, we propose a new concept of a spaceborne antenna array, i.e., a flexible coilable array with resilient spiral antennas which behave linear

polarization and has a low strain under the compression, as shown in Figure 1. This coilable array has advantages such as high shape accuracy and deployment and small impact and vibration, which has not been used on satellites at present.

When the flexible coilable antenna array is coiling, the conical spiral antenna would be compressed and combined with coilable membrane. There may be two extremely unfavorable deformation conditions at this time. When the thickness of the coilable membrane is too large, the membrane is too rigid to roll and also overweight. On the other hand, when the thickness of the membrane is too small, the membrane is too compliable to compress conical spiral antennas on the surface of the scroll. Therefore, a theoretical model is essential to determine the minimum thickness required for the coilable membrane to fully compress the conical spiral antenna and to achieve lightweight design of membrane to optimize the launching cost. However, during the coiling process, the conical spiral antenna from the outer ring to the inner ring gradually contacts the bottom surface of membrane. The conical spiral antenna has a complex, large deformation and displacement, exhibiting significant nonlinearity [25–28]. It remains challenging to model the mechanics design of conical spiral antenna for flexible coilable antenna array. The widely used close-coiled spring theory and sparse-coiled spring theory are only suitable for small deformation in the linear elastic regime [29–33]. In addition, there are some nonlinear theories in consideration of the change of the helix angle [34–37]. However, the constraint of the underlying membrane on the deformation of the spring structure is not considered, such that these models cannot be applied to the coiling process. Finite element models were adopted to obtain the deformation process of a general conical spiral antenna [38–41] but could not lead to any analytical solution or scaling law [42–44]. It is of great significance to the lightweight design and mechanical design of the flexible coilable antenna array.

This paper is arranged as follows: the coiling behavior of the flexible coilable antenna array with conical spiral antennas is studied. The deformation between the coilable membrane and the spiral antenna is deduced during the coiling process. The finite element method and the phototype are used to verify the accuracy of the theoretical derivation. This provides modeling and numerical support and theoretical guidance for the design of conical spiral antenna and the selection of membrane thickness.

2. Structural Model of the Flexible Coilable Antenna Array

Figure 1 shows a schematic diagram of flexible coilable antenna array with three-dimensional (3D) conical spiral antennas during the coiling process. The coilable antenna array is mainly composed of a feed, a flexible coilable membrane, and several conical spiral antennas. A large number of conical spiral antennas are uniformly distributed on the coilable membrane. One end of the conical spiral antenna is fixedly connected with the coilable membrane, and the other end is traction-free. The membrane is rolled up by a drive

motor to compress the coilable antenna array and press it on the scroll, as shown in Figure 1(b). After the coilable antenna array enters its orbit, the coilable membrane rotates in the opposite direction and unfolds such that the antennae return to the original 3D state due to elasticity, as shown in Figure 1(d).

For ease of analyzing the mechanical behavior of the coilable antenna array, this antenna model would be simplified as coilable membrane with conical spiral antenna. During the coiling process, the straight portion of the coilable membrane (see Figure 1(d)) has rigid-body displacement in the horizontal direction without deformation. The coiled portion presses and deforms the spiral antenna. The conical spiral antenna is a tubular structure fabricated by highly elastic material. The inner cavity of the conical spiral tube (typical diameter is greater than 1 mm) is arranged with a metal wire as a radiating element (typical diameter is less than 0.2 mm). The mechanical behavior of the spiral tube is considered at this time since the metal wire is thin.

At the moment of contact, the height H of the antenna and the radius R_r of the scroll are related geometrically via (see Figure 2(a))

$$2 \sin^2 \frac{\alpha}{2} = \frac{H}{R_r}. \tag{1}$$

To ensure that the conical spiral antenna can be flattened rather than tipped during the coiling process, the contract angle α between the antenna and the membrane should be close to zero for a vertical pressing. Given the height of the conical spiral antenna, this requires the radius of the scroll to be sufficiently large, so that the height of the conical spiral antenna is much smaller than the radius of the scroll. Therefore, the interaction between the coilable membrane and one conical spiral antenna can be regarded as the vertical force applied by two planar membranes.

Figures 2(b) and 2(c) show the cross section of the conical spiral antenna, which define geometric parameters of the flexible coilable antenna array. Thickness of the coilable membrane is defined as b_m. R_r represents the radius of the scroll. Pitch of the conical spiral antenna is defined as t. R_n and R_1 are the upper and lower radius of the conical spiral antenna. From the biggest layer to the smallest layer for the radius of the conical spiral antenna, it numbers as 1, 2, i, and n, successively. d is the diameter of the conical spiral antenna. b is the ratio of the inner and outer diameter of the conical spiral antenna. L is the total length of the conical spiral antenna, which is equal to $n\pi(R_1 + R_n)$. The radius of the ith layer is $R_i = R_1 - i/n(R_1 - R_n)$.

3. Mechanical Behavior of Conical Spiral Antenna

For the spiral antenna to be fully flattened in the coiling process, the membrane rigidity needs to be much larger than the antenna rigidity, such that the membrane deformation is much smaller than the antenna deformation. Therefore, the mechanical behaviors of the conical spiral antenna can be analyzed without consideration of the membrane
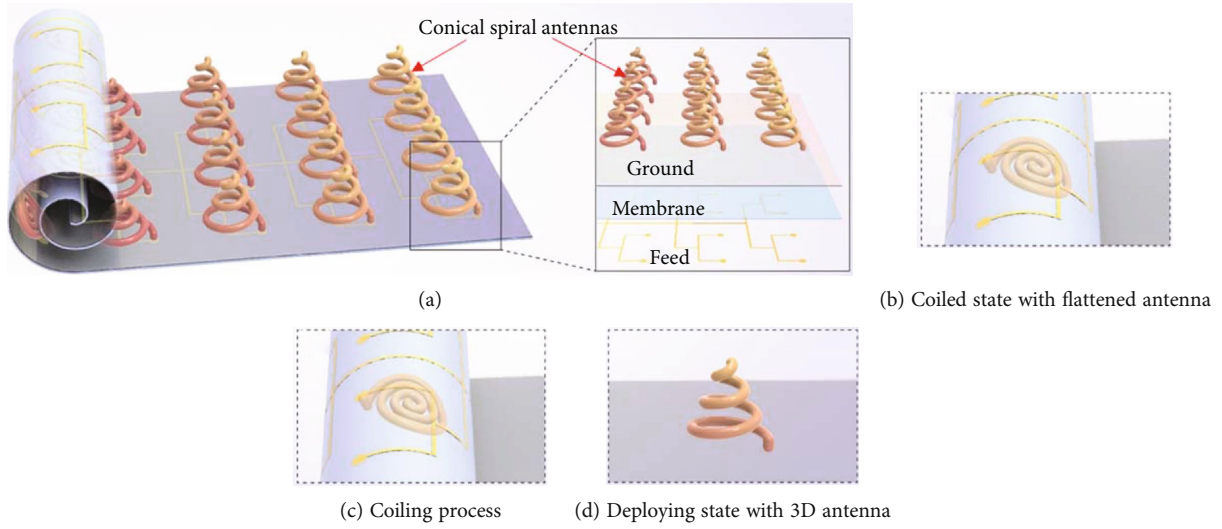
(a)

(b) Coiled state with flattened antenna

(c) Coiling process

(d) Deploying state with 3D antenna

FIGURE 1: Schematic illustration of flexible coilable antenna array with conical spiral antenna.
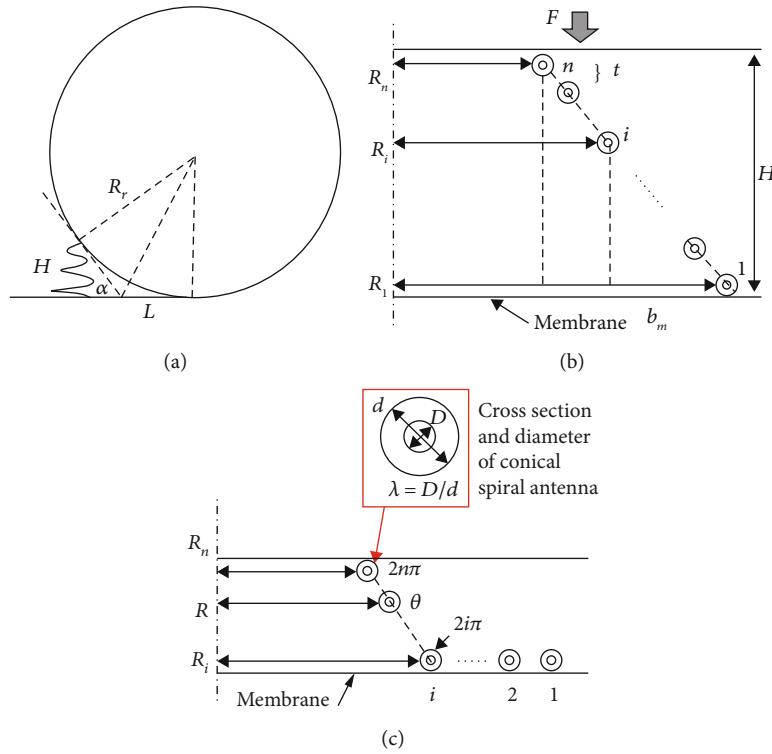

(a)

(b)

(c)

FIGURE 2: (a) Geometric relationship between scroll and conical spiral antenna. (b) Cross section of conical spiral antenna at the initial state. (c) Cross section of conical spiral antenna under partial compression.

deformation. The bottom end of the conical spiral antenna is fixedly connected to the bottom of coilable membrane, and the contact force F from the top membrane is applied vertically on the top end. During the compressive process, the bottom of the spiral antenna would be in contact with the coilable membrane of the antenna and no longer separate.

Because the conical spiral antenna has a small helix angle, the deformation is dominated by torsion. It is different for the force required to flatten each layer of the conical spiral antenna. Initially, for a small deformation, the displacement of the antenna at the contact position, induced by the contact force, can be obtained analytically as

$$\delta = \int_0^L \frac{F \cdot R^2}{GI_p} ds = \int_{R_n}^{R_1} \frac{2\pi F R^3 n}{GI_p (R_1 - R_n)} dR = \frac{n\pi F \left(R_1^{\,4} - R_n^{\,4}\right)}{2GI_p (R_1 - R_n)},$$

(2)

where a polar angle θ of the conical spiral antenna goes downward from the smallest to the biggest for the radius. $ds = Rd\theta = (2\pi nR/R_1 - R_n)dR$ is the derivative of the conical spiral antenna. G is the shear modulus. $I_p = \pi d^4 (1 - \lambda^4)/32$

is the polar moment of inertia of the hollow circular section with respect to center of circle for the conical spiral antenna. $\lambda = D/d$ is the ratio of inside and outside diameters of the tube.

The stiffness in the ith layer for the conical spiral antenna can be expressed as $k_i = GI_p/\pi R_i^3$ based on the torsional theory with small deformation. When the force exceeds a critical value,

$$F_1 = \frac{tGI_p}{2\pi R_1^3}. \tag{3}$$

The first layer before all others of the spiral antenna is fully flattened on the membrane and no longer has displacement. At this moment, the displacement at the contact position with the membrane is t. When the pressing force further increases, the model can be regarded as a spring with outer radius R_2 replacing R_1 in the previous analysis. In general, the displacement can be obtained similarly as

$$\delta = i \cdot t + \frac{n\pi F(R_i^4 - R_n^4)}{2GI_p(R_1 - R_n)} = \frac{n}{R_1 - R_n}\left[\frac{\pi F}{2GI_p}(R_i^4 - R_n^4) + t(R_1 - R_i)\right]. \tag{4}$$

The maximum force required to flatten all layers of the conical spiral antenna is

$$F_0 = \frac{tGI_p}{2\pi R_n^3}. \tag{5}$$

Based on Equation (6), the normalized displacement $nt - \delta/nt$ can be expressed in terms of normalized force F/F_0 as

$$\left(\frac{nt - \delta}{nt}\right)\left(\frac{R_1}{R_n} - 1\right) = \frac{3}{4}\left(\frac{F_0}{F}\right)^{1/3} + \frac{F}{4F_0} - 1. \tag{6}$$

Equation (6) illustrates that the maximum compressive force is closely related to the third power of the minimum radius of the conical spiral antenna. Equation (7) gives the quantitative relationship between normalized force and displacement during compression. At the initial stage of compression, the force on the conical spiral antenna is linearly proportional to its displacement. When F approaches F_0, the normalized force increases rapidly with the normalized displacement. The stiffness of the conical spiral antenna increases during the entire compressive process.

Numerical simulation is performed to validate the above analytical model. Several 3D geometric models of the conical spiral antenna are established in different geometric parameters (G, t, d, R_1, R_n, etc.) by using a modeling software UG. The finite element model of the conical spiral antenna is established by using the commercial software ABAQUS. The upper and lower membranes are defined by analytical rigid body, as shown in Figures 2(b) and 2(c). And there is a friction between the top of the antenna and the upper membrane. The beam element is applied to the coilable antenna model. Hence, there is a complex nonlinear contact

between the conical spiral antenna and the membrane in the numerical model, making it difficult to predict the maximum force. When the conical spiral is fully flattened, it has a great effect on the convergence and accuracy of the numerical results. Therefore, the corresponding force extracted as a comparison, when the normalized displacement is 60-90%. As shown in Figure 3, the force and displacement in the theoretical solution are validated by finite element analysis (FEA) without any parameter fitting, for the conical spiral antenna with polypropylene (PP) material. The baseline for the geometrical and material parameters of conical spiral antenna are $E = 890$ MPa, $d = 1$ mm, $\lambda = 0.2$, $R_1 = 2.5$ mm, $R_n = 14$ mm, $t = 4$ mm, and $n = 5$. The parameter $(1 - \delta/nt)(R_1/R_n - 1)$ has a large of range.

It can be seen that there is a high nonlinearity between the normalized force and displacement in the conical spiral antenna. It is shown that, through the numerical analysis, the changes of geometric parameters for the conical spiral antenna have no effect on the nonlinear relationship. It is proved that numerical results are highly consistent with the theoretical results. Therefore, this derived theory can be used to estimate the compressive force and displacement. In turn, it can be used for the design of conical spiral antenna structure yet.

4. Thickness of Coilable Membrane

The foregoing studies have investigated the deformation behavior of the conical spiral antenna under the force applied by two parallel membranes. Dozens of conical spiral antennas are periodically arrayed on the coilable membrane in both the circumferential and the axial directions, where the spacing between adjacent antennas is defined as w_1 and w_2, respectively. As the spacing is much smaller than the membrane size, the period force F applied by the conical spiral antenna on the rolled membrane is equivalent to a uniform pressure $P = F/w_1 \cdot w_2$ in both circumferential and axial directions. The larger the diameter of the scroll, the greater the thickness (b_m) of the membrane can be wound. The increasing thickness magnifies the rigidity of the membrane itself, and the total weight of the antenna increases at the same time. To optimize the flight cost of the spacecraft, it is necessary to determine the minimum thickness required by the coilable membrane to fully compress the antenna.

For the pressure P applied by the conical spiral antenna much smaller than the elastic modulus (E_m) of membrane, i.e., $P \ll E_m$, the induced membrane deformation (ΔR_r) is small and linearly elastic, as shown in Figure 4. The Poisson's ratio of the membrane is defined as ν_m. The stress in circumferential direction of the membrane can be obtained from force balance as

$$\sigma_\varphi = \frac{P \cdot 2\pi R_r W_m}{2 \cdot b_m W_m} = \frac{P \cdot \pi R_r}{b_m}. \tag{7}$$

Noticing that the strain in radial direction is negligible for a membrane with small thickness, the membrane deformation is
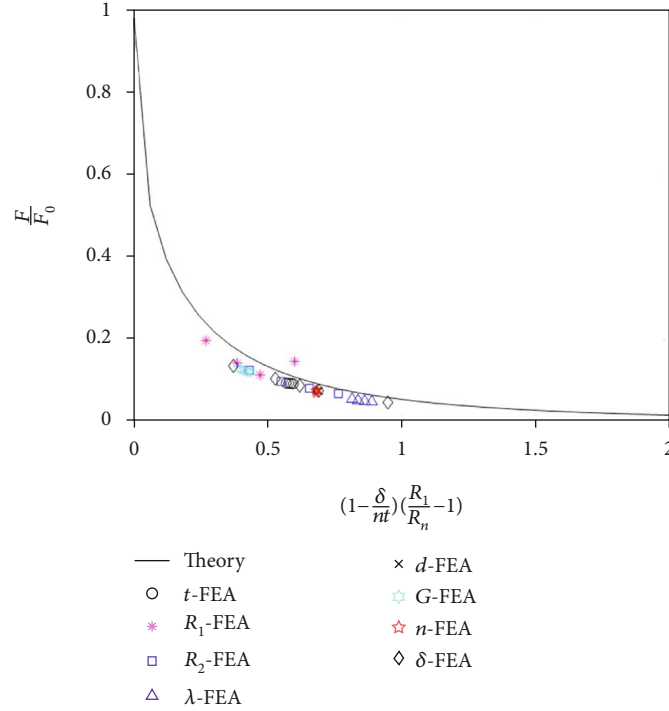
FIGURE 3: Theoretical and finite element analysis (FEA) results of the normalized force F/F_0 vs. normalized displacement $(1 - \delta/nt)(R_1/R_2 - 1)$ relationship in different geometric parameters (G, t, d, R_1, R_2, n, and δ).
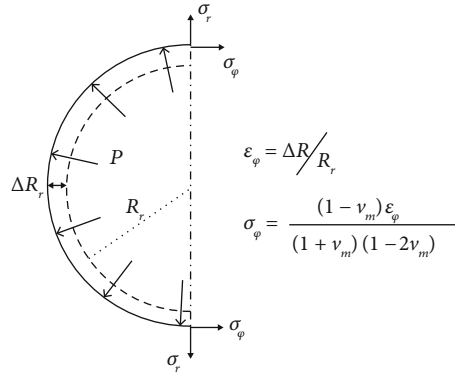

FIGURE 4: Schematic illustration of the membrane deformation after coiling.

$$\frac{\Delta R}{R_r} = \varepsilon_\varphi = \frac{\pi R_r P \left(1 - v_m - 2v_m{}^2\right)}{E_m \cdot b_m \cdot (1 - v_m)}. \tag{8}$$

When the conical spiral antennas are fully flattened, the membrane deformation is equal to the cross-sectional diameter of the conical spiral structure, i.e., $\Delta R = d$, and a pressure applied by the membrane with thickness b_m is $E_m d b_m (1 - v_m)/\pi R_r^2 (1 - v_m - 2v_m{}^2)$. According to Equation (6), the pressure needs to be larger than $tGI_p/2\pi w_1 \cdot w_2 R_n^3$ for the membrane to fully flatten the antenna, i.e.,

$$\frac{E_m d b_m (1 - v_m)}{\pi R_r^2 \left(1 - v_m - 2v_m{}^2\right)} \geq \frac{tGI_p}{2\pi w_1 \cdot w_2 R_n^3}. \tag{9}$$

Hence, with the other parameters given, the required thickness of the membrane is

$$b_m > b_{\min} = \frac{tGI_p R_r^2 \left(1 - v_m - 2v_m{}^2\right)}{2w_1 w_2 d E_m R_1^3 (1 - v_m)}. \tag{10}$$

The minimum thickness $b_{\min}$ of the membrane can be calculated, which is related to the geometrical and material parameters and the arrangement density of the conical spiral antenna. Taking the C-band conical spiral antenna with polymer as an example, the geometrical and material parameters of conical spiral antenna and membrane and the calculated minimum thickness $b_{\min}$ are shown in Table 1. Finally, one prototype for flexible coilable antenna array with conical spiral antennas is fabricated as shown in Figure 5. The

TABLE 1: Parameters of membrane and conical spiral antenna.

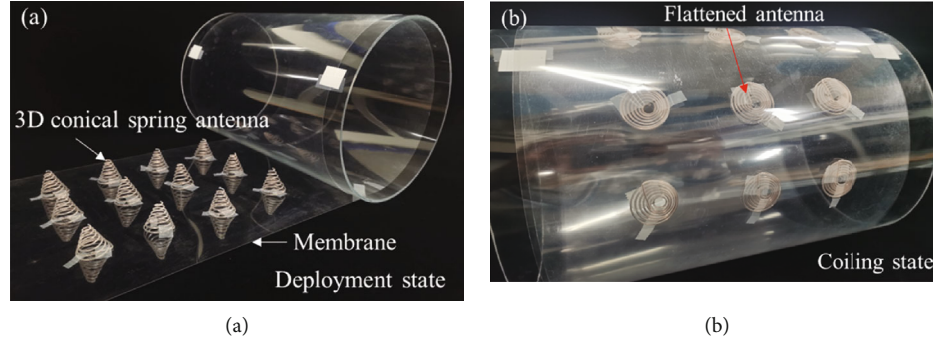| Antenna, membrane	v, v_m	t (mm)	E, E_m (MPa)	d (mm)	R_r (mm)	w_1, w_2 (mm)	R_1 (mm)	b_m (mm)
PP, PET	0.42, 0.32	4	890, 4000	1	100	40, 40	2	0.018
PI, PI	0.34, 0.34	4	4000, 4000	1	100	40, 40	2	0.087

(a)   (b)

FIGURE 5: Prototype of the fabricated flexible coilable antenna array.

thickness of the coilable membrane fabricated by polyethylene terephthalate (PET) is 0.1 mm, and the diameter of conical spiral antenna fabricated by polypropylene (PP) is 1 mm. Twelve conical spiral antennas are periodically arrayed on the coilable membrane in both the circumferential direction with 50 mm and the axial direction with 50 mm. The radius of scroll is 75 mm. Under the action of the membrane, the conical spiral antennas can be fully flattened and resiled during the coiling and outspreading processes, separately, as shown in Figure 5.

5. Conclusion

The flexible coilable antenna array with conical spiral antenna is a brand new spaceborne array. This paper investigates mechanical behavior of the flexible coilable antenna array during the coiling process. A theoretical relationship of the conical spiral antenna is given between normalized force and displacement, which exhibits a high nonlinear behavior. FEA is performed to validate the above theoretical model. Furthermore, the thickness of the coilable membrane to fully flatten the antenna can be predicted by an analytical solution about the geometrical and material parameters between the coilable membrane and the conical spiral antenna. This research provides important theoretical support for the design and fabrication of the flexible coilable antenna array with conical spiral antennas.

Data Availability

The data used to support the findings of this study are included within the article.

Conflicts of Interest

The authors declare that there are no conflicts of interest regarding the publication of this paper.

References

[1] Z. Xie, R. Avila, Y. Huang, and J. A. Rogers, "Flexible and stretchable antennas for biointegrated electronics," *Advanced Materials*, vol. 32, no. 15, p. 1902767, 2020.

[2] Y. Zhang, D. C. Castro, Y. Han et al., "Battery-free, lightweight, injectable microsystem for in vivo wireless pharmacology and optogenetics," *Proceedings of the National Academy of Sciences*, vol. 116, no. 43, pp. 21427–21437, 2019.

[3] Z. Xie, B. Ji, and Q. Huo, "Mechanics design of stretchable near field communication antenna with serpentine wires," *Journal of Applied Mechanics -Transactions of the ASME*, vol. 85, no. 4, 2018.

[4] S. Kanaparthi, V. R. Sekhar, and S. Badhulika, "Flexible, eco-friendly and highly sensitive paper antenna based electromechanical sensor for wireless human motion detection and structural health monitoring," *Extreme Mechanics Letters*, vol. 9, pp. 324–330, 2016.

[5] C. Wang, Y. Wang, P. Lian et al., "Space phased array antenna developments: a perspective on structural design," *IEEE Aerospace and Electronic Systems Magazine*, vol. 35, no. 7, pp. 44–63, 2020.

[6] H. Fang, M. Lou, J. Huang, L. Hsia, and G. Kerdanyan, "Design and development of an inflatable reflectarray antenna," *IPN Progress Report*, vol. 149, pp. 1–18, 2002.

[7] H. Wang, D. Zhao, Y. Jin, M. Wang, T. Mukhopadhyay, and Z. You, "Modulation of multi-directional auxeticity in hybrid origami metamaterials," *Applied Materials Today*, vol. 20, p. 100715, 2020.

[8] H. Yang, H. Guo, Y. Wang, J. Feng, and D. Tian, "Analytical solution of the peak bending moment of an M boom for membrane deployable structures," *International Journal of Solids and Structures*, vol. 206, pp. 236–246, 2020.

[9] S. Zhang, J. Du, B. Duan, G. Yang, and Y. Ma, "Integrated structural–electromagnetic shape control of cable mesh reflector antennas," *AIAA Journal*, vol. 53, no. 5, pp. 1395–1399, 2015.

[10] P. K. C. Wang and J. C. Sarina, "Control of reflector vibrations in large spaceborne antennas by means of movable dampers," *Journal of Applied Mechanics-Transactions of the Asme*, vol. 50, no. 3, pp. 669–673, 1983.

[11] Y. Liu, F. Pan, B. Ding, Y. Zhu, K. Yang, and Y. Chen, "Multi-stable shape-reconfigurable metawire in 3D space," *Extreme Mechanics Letters*, vol. 50, article 101535, 2022.

[12] Y. Rahmat-Samii and R. Haupt, "Reflector antenna developments: a perspective on the past, present and future," *IEEE Antennas and Propagation Magazine*, vol. 57, no. 2, pp. 85–95, 2015.

[13] Z. M. Xia, C. G. Wang, and H. F. Tan, "Quasi-static unfolding mechanics of a creased membrane based on a finite deformation crease–beam model," *International Journal of Solids and Structures*, vol. 207, pp. 104–112, 2020.

[14] S. Yang and C. Sultan, "Deployment of foldable tensegrity-membrane systems via transition between tensegrity configurations and tensegrity-membrane configurations," *International Journal of Solids and Structures*, vol. 160, pp. 103–119, 2019.

[15] X. Wu, R. Cheng, T. H. T. Chan, G. Liu, and J. Xia, "Algorithm for rapidly predicting the worst surface accuracy of deployable mesh reflectors," *Applied Mathematical Modelling*, vol. 98, pp. 229–244, 2021.

[16] S. H. Eedala, S. Elakiyaa, R. Nethra, R. Asha, and M. Jayakumar, "Design of helical array antenna based ground terminal for satellite communication on the move," in *4th International Conference on Electronics, Communication and Aerospace Technology*, Coimbatore, India, Nov. 2020.

[17] J. Jiang, L. Zhang, N. Luo et al., "An ultra-wideband stacked spiral-helix composite antenna," in *14th European Conference on Antennas and Propagation*, Copenhagen, Denmark, March 2020.

[18] M. A. Elmansouri, J. B. Bargeron, and D. S. Filipovic, "Ultra-wideband spiral-helix antenna array," in *Antennas and Propagation Society International Symposium*, Memphis, TN, USA, July 2014.

[19] X. Meng, B. Liu, Y. Wang, T. Zhang, and J. Xiao, "Third-order polynomials model for analyzing multilayer hard/soft materials in flexible electronics," *Journal of Applied Mechanics-Transactions of the Asme*, vol. 83, no. 8, 2016.

[20] K. Sim, S. Chen, Z. Li et al., "Three-dimensional curvy electronics created using conformal additive stamp printing, Nature," *Electronics*, vol. 2, no. 10, pp. 471–479, 2019.

[21] C. Wang, S. Zhang, S. Nie, Y. Su, W. Chen, and J. Song, "Buckling of a stiff thin film on a bi-layer compliant substrate of finite thickness," *International Journal of Solids and Structures*, vol. 188-189, pp. 133–140, 2020.

[22] T. Li and Z. Suo, "Deformability of thin metal films on elastomer substrates," *International Journal of Solids and Structures*, vol. 43, no. 7-8, pp. 2351–2363, 2006.

[23] M. R. M. Hashemi, A. C. Fikes, M. Gal-Katziri et al., "A flexible phased array system with low areal mass density, Nature," *Electronics*, vol. 2, no. 5, pp. 195–205, 2019.

[24] Y. Han, K. Hu, R. Zhao et al., "Design of combined printed helical spiral antenna and helical inverted-f antenna for unmanned aerial vehicle application," *IEEE Access*, vol. 8, pp. 54115–54124, 2020.

[25] M. Wu and W. Hsu, "Modelling the static and dynamic behavior of a conical spring by considering the coil close and damping effects," *Journal of Sound and Vibration*, vol. 214, no. 1, pp. 17–28, 1998.

[26] V. Yildirim, "A parametric study on the free vibration of non-cylindrical helical springs," *Journal of Applied Mechanics-Transactions of the Asme*, vol. 65, no. 1, pp. 157–163, 1998.

[27] Y. Luxenburg and S. Givli, "The static response of axisymmetric conical shells exhibiting bistable behavior," *Journal of Applied Mechanics-Transactions of the Asme*, vol. 88, no. 11, 2021.

[28] R. Mirzaeifar, R. DesRoches, and A. Yavari, "A combined analytical, numerical, and experimental study of shape-memory-alloy helical springs," *International Journal of Solids and Structures*, vol. 48, no. 3-4, pp. 611–624, 2011.

[29] T. Iritani, A. Shozaki, B. Sheng, M. Sugimoto, T. Okazaki, and M. Aketa, "70 Prediction of the dynamic characteristics in valve train design of a diesel engine," *SAE Transactions*, vol. 111, pp. 1–7, 2002.

[30] F. C. Grant, "Energy analysis of the conical-spring oscillator," *American Journal of Physics*, vol. 54, no. 3, pp. 227–233, 1986.

[31] M. Paredes and E. Rodriguez, "Optimal design of conical springs," *Engineering with Computers*, vol. 25, no. 2, pp. 147–154, 2009.

[32] B. Zhou, Z. Wang, and S. Xue, "Mechanical model for super-elastic helical spring of shape memory alloy, Journal of," *Mechanical Engineering*, vol. 55, no. 8, pp. 56–64, 2019.

[33] E. Rodriguez, M. Paredes, and M. Sartor, "Analytical behavior law for a constant pitch conical compression spring," *Journal of Mechanical Design-Transactions of the ASME*, vol. 128, no. 6, pp. 1352–1356, 2006.

[34] Y. He, G. Zou, X. Pan, F. Zhang, and W. He, "Nonlinear theory and experimental study of helical spring," *Engineering Mechanics*, vol. 14, pp. 56–61, 1994.

[35] L. Hong, H. Yunzeng, and Y. Lihong, "Nonlinear theory of conical helical spring," *Journal of Harbin Engineering University*, vol. 26, pp. 628–632, 2005.

[36] J.-S. Chen and I. S. Chen, "Deformation and vibration of a spiral spring," *International Journal of Solids and Structures*, vol. 64-65, pp. 166–175, 2015.

[37] N. V. Viet, W. Zaki, R. Umer, and Y. Xu, "Mathematical model for superelastic shape memory alloy springs with large spring index," *International Journal of Solids and Structures*, vol. 185-186, pp. 159–169, 2020.

[38] Z. Sen, C. Shaofeng, W. Huanding, and Q. Ting, "Finite element analysis of spatial curved beam in large deformation," *Journal of Southeast University*, vol. 26, pp. 591–596, 2010.

[39] T. Meilan, W. Xinwei, and Z. Yong, "An efficient finite element of spatial curved beams, Chinese Journal of," *Computational Mechanics*, vol. 1, pp. 78–82, 2005.

[40] D. F. Lalo, M. Greco, and M. Meroniuc, "Numerical modeling and experimental characterization of elastomeric pads bonded in a conical spring under multiaxial loads and pre-compression," *Mathematical Problems in Engineering*, vol. 2019, 14 pages, 2019.

[41] J. Zhang, Z. Qi, Y. Zhuo, and S. Guo, "Stiffness analysis of helix spring using exact geometric beam element," *Engineering Mechanics*, vol. 37, p. 16, 2020.

[42] K. Zhou and F. Xiao, "Contact simulation of cylindrical helical spring based on Ansys," *Mechanical Engineering & Automation*, vol. 212, pp. 60–64, 2019.

[43] X. Yuan, S. M. Won, M. Han et al., "Mechanics of encapsulated three-dimensional structures for simultaneous sensing of pressure and shear stress," *Journal of the Mechanics and Physics of Solids*, vol. 151, article 104400, 2021.

[44] S. Li, M. Han, J. A. Rogers, Y. Zhang, Y. Huang, and H. Wang, "Mechanics of buckled serpentine structures formed via mechanics-guided, deterministic three-dimensional assembly," *Journal of the Mechanics and Physics of Solids*, vol. 125, pp. 736–748, 2019.